Charge and Solvent Effects on the Redox Behavior of Vanadyl Salen-Crown Complexes

Hien M. Nguyen,[a] *Harry W. T. Morgan,*[b] *Teera Chantarojsiri,*[c] *Tyler A. Kerr,*[a] *Jenny Y. Yang,*[a] *Anastassia Alexandrova,**[,b] *Nadia G. Léonard**[,a]

[a] Department of Chemistry, University of California, Irvine, California, 92697, United States

[b] Department of Chemistry and Biochemistry, University of California, Los Angeles, California 90095, United States

[c] Department of Chemistry and Center of Excellence for Innovation in Chemistry, Faculty of Science, Mahidol University, Bangkok, 10400, Thailand

ABSTRACT. The incorporation of charged groups proximal to a redox active transition metal center is an attractive strategy for altering redox behavior, installing electric fields, and enhancing catalysis. Vanadyl salen (salen = *N,N'*-ethylenebis(salicylideneaminato)) complexes functionalized with a crown ether containing a non-redox active Lewis acidic metal cation (**V-Na**, **V-K**, **V-Ba**, **V-La**, **V-Ce**, and **V-Nd**) were synthesized. The electrochemical behavior of this series of complexes was investigated by cyclic voltammetry in solvents with varying polarity and dielectric constant (ε) (acetonitrile, ε = 37.5; *N,N*-dimethylformamide, ε = 36.7; and dichloromethane, ε = 8.93). The vanadium(V/IV) reduction potential shifted anodically (>900 mV in acetonitrile and >700 mV in dichloromethane) with increasing cation charge as compared to

complexes lacking the proximal cation. The reduction potential for all vanadyl salen-crown complexes measured in *N*,*N*-dimethylformamide was insensitive to cation charge magnitude, regardless of electrolyte or counter anion used. Titration studies of *N*,*N*-dimethylformamide into acetonitrile resulted in cathodic shifting of the vanadium(V/IV) reduction potential with increasing concentration of *N*,*N*-dimethylformamide. Binding constants of *N*,*N*-dimethylformamide ($\log(K_{DMF})$) for the series of crown complexes show increased binding affinity in the order of **V-La>V-Ba>V-K>(salen)V(O)**, indicating an enhancement of Lewis acid/base interaction with increase of cation charge. The redox behavior of **(salen)V(O)** and **(salen-OMe)V(O)** (salen-OMe = *N*,*N'*-ethylenebis(3-methoxysalicylideneamine) was also investigated and compared to the crown-containing complexes. For **(salen-OMe)V(O)**, a weak association of triflate salt at the vanadium(IV) oxidation state was observed through cyclic voltammetry titration experiments and cation dissociation upon oxidation to vanadium(V) was identified. These studies demonstrates the non-innocent role of solvent coordination and cation/anion effects on redox behavior.

INTRODUCTION.

Vanadim(IV) and vanadium(V) complexes are attractive to study due to their activity for a variety of oxidation reactions.[1–3] Vanadyl complexes, those possessing a vanadium–oxygen multiple bond, dominate the chemistry of vanadium due to their stability, which has led to many applications ranging from catalysis,[4–14] electrochemistry,[15,16] bioinorganic chemistry,[17–22] and molecular magnetism.[23–28] Specifically, salen (salen = *N*,*N'*-ethylenebis(salicylideneaminato)) vanadyl complexes have shown activity for the oxygen reduction reaction (ORR)[29] and autoxidation of alkenes.[30] Given the rich oxidation chemistry of vanadyl salen complexes, tuning the electrochemistry and redox behavior is useful for controlling their reactivity at very oxidizing

potentials. Further, it is important to understand solvent effects on the redox behavior, as this may determine reactivity profiles and stability of the vanadyl ion. Proximal non-redox active Lewis acidic metals have been shown to shift redox potentials and enhance reactivity.[31–35] Increasing the magnitude of charge of a positively charged ion or substituent typically results in an anodic shift (positive shift) of reduction potential. Investigations on charge effects on homogeneous transition metal complexes are important for understanding electron transfer processes, spectroscopic properties, and impact on catalytic activity.[36–38] Given the reversibility of the vanadyl (V/IV) redox couple and its role in reactions involving vanadium salen complexes, we investigated vanadyl salen-crown complexes containing various non-redox active cations to modify the redox properties. Solvents with varying polarity and dielectric constant (ε) (acetonitrile, ε = 37.5; *N*,*N*-dimethylformamide, ε = 36.7; and dichloromethane, ε = 8.93) were investigated to explore how both charge and solvent affect electron transfer, reorganization, and coordination around the vanadyl center. Gaining a better understanding of the interplay of charge effects, solvent interactions, and redox behavior at vanadyl complexes informs how these characteristics influence reactivity.

Chart 1. Vanadyl complexes investigated in this study.

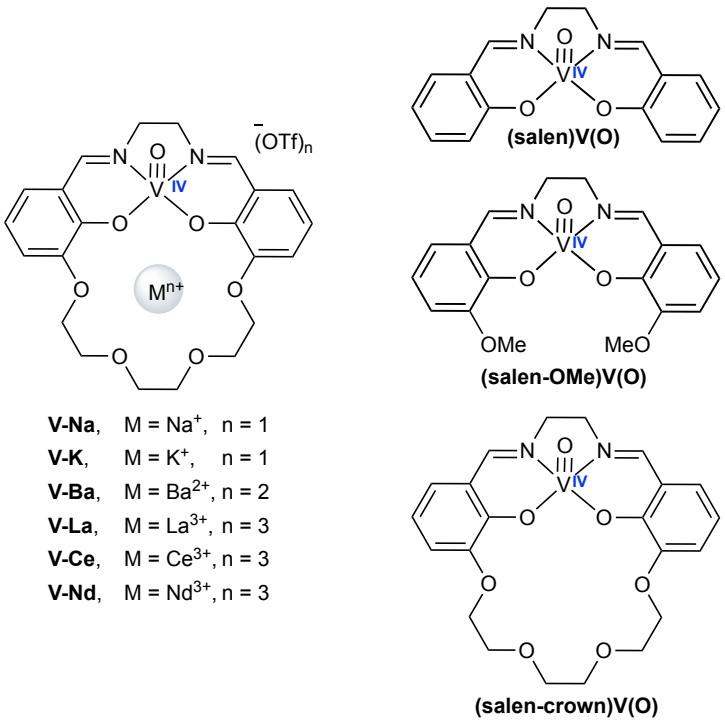

RESULTS AND DISCUSSION.

Synthesis and structural characterization. The **salen-crown**[39] and **salen-crown-M**[31–33,40] ($M = Na^+$, K^+, Ba^{2+}) ligands have been previously reported and were prepared accordingly. **Salen-crown-Ln** ligands ($Ln = La^{3+}$, Ce^{3+}, Nd^{3+}) were prepared through metalation of **salen-crown** with the respective $Ln(OTf)_3$ salt in a 1:1 mixture of chloroform and methanol. The corresponding vanadyl complexes, **V-M** ($M = Na^+$, K^+, Ba^{2+}, Nd^{3+}, La^{3+}), were then isolated following metalation of the desired **salen-crown-M** ligand with $V(acac)_3$ (acac = acetylacetonate) in ethanol followed by exposure to air. Alternatively, the desired vanadyl complexes could be obtained directly through metalation of the **salen-crown-M** ligand with vanadyl acetylacetonate ($V(O)(acac)_2$) (Scheme 1). Single crystals suitable for X-ray diffraction of the vanadyl complexes (**V-Na**, **V-K**, **V-Ba**, **V-La**, **V-Ce**, **V-Nd**) were obtained following slow diffusion of diethyl ether into concentrated acetonitrile

solutions at room temperature (Figure 1). Attempts to obtain X-ray quality crystals of the empty crown vanadyl complex (**(salen-crown)V(O)**) through slow diffusion of diethyl ether into either acetonitrile or *N*,*N*-dimethylforamide solutions were unsuccessful. Complexes **(salen)V(O)** and **(salen-OMe)V(O)** were prepared according to previously reported procedures.[41]

Scheme 1. Synthesis of vanadyl complexes.

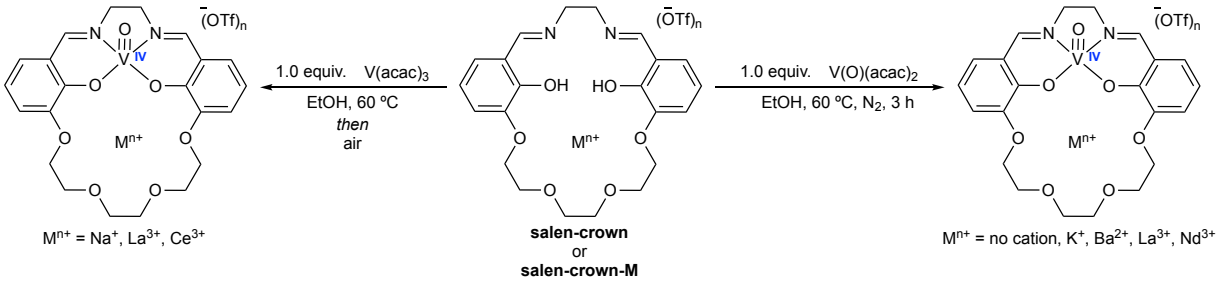

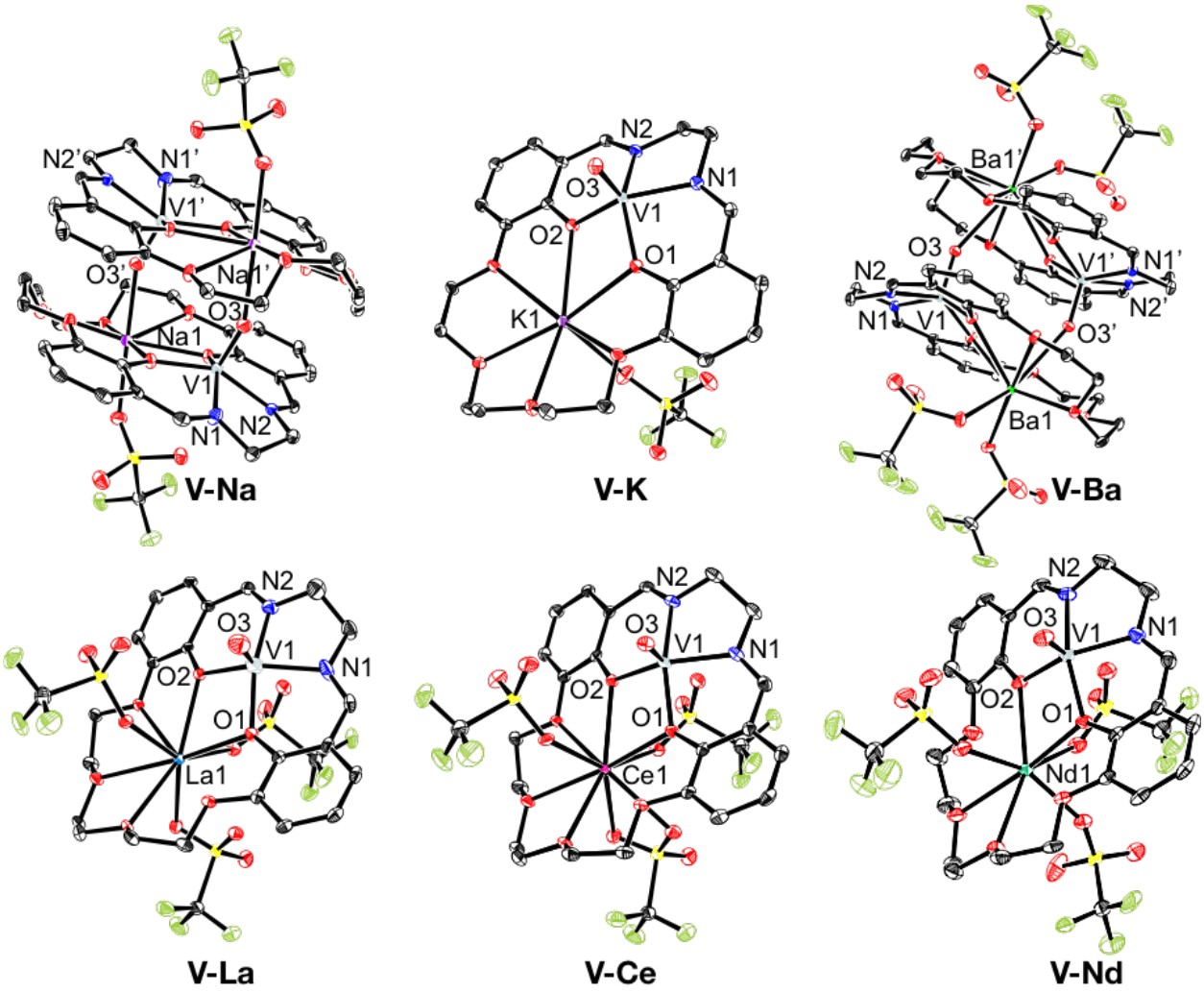

Figure 1. Solid-state molecular structures of vanadyl complexes at 50% probability ellipsoids. Hydrogen atoms omitted for clarity. See Table 1 for selected bond metrics.

In the solid state, **V-Na** and **V-Ba** complexes exist as dimers where the oxo ligand bridges between the vanadium and cation, M (M = Na^+ or Ba^{2+}). The bond lengths of the V–O bonds vary minimally across the series for the solid state monomeric or dimeric species (Table 1). Direct binding of a Lewis acid to an oxo-metal fragment has been shown to result in significant elongation of the M–O bond.[42–44] For the crown complexes presented here we observe a slight increase in the V–O bond lengths for **V-Na**, **V-K**, **V-Ba**, and **V-La**, but the V–O bond lengths of **V-Ce** and **V-Nd** are within error of the V–O length for **(salen-OMe)V(O)**. All complexes exhibit distorted square

pyramidal geometry with τ_5 values ranging between 0.01 and 0.14. The vanadium atom is displaced toward the apical oxygen atom away from the basal plane (defined by the salen N_2O_2 atoms) in all complexes. The **V-Nd** compound had significant disorder in the crystal structure.

Table 1. Summary of structural parameters of vanadyl complexes.

Complex	**V–O Bond (Å)**	**V–M distance (Å)**	**Cation M radius (Å)[a]**	τ_5	**Displacement of V from basal plane (N_2O_2) (Å)**
(salen)V(O)[b]	1.590(1)	–	–	0.18	0.589
(salen-OMe)V(O)[c]	1.590(3)	–	–	0.13	0.589
V-Na	1.5986(15)	3.4850(10)	1.02	0.01	0.518
V-K	1.6025(10)	3.8076(4)	1.38	0.14	0.613
V-Ba	1.6059(11)	3.7983(3)	1.35	0.12	0.610
V-La	1.600(3)	3.5980(7)	1.03	0.12	0.492
V-Ce	1.588(2)	3.6100(6)	1.01	0.10	0.485
V-Nd	1.586(3)	3.59569(17)	0.98	0.10	0.492

[a] Values from ref. [45]. [b] Values from ref. [46]. [c] Values from ref. [47].

Cyclic voltammetry. Cyclic voltammetry experiments for the series of vanadyl complexes were conducted in solvents of varying polarity as measured by the solvents' dielectric constants (ε). Acetonitrile (MeCN) and *N,N*-dimethylformamide (DMF) have similar dielectric constants of 37.5 and 36.7, respectively, and dichloromethane (DCM) has a dielectric constant of 8.93.[48] Understanding solvent effects when charge is present is also critical for ion-pairing and solvent screening as it relates to reactivity.[49] Cyclic voltammograms of **(salen)V(O)** (Figure 2, black trace) and **(salen-OMe)V(O)** (Figure 2, gray trace) exhibit a reversible redox feature at 0.090 and 0.066 V vs $(C_5H_5)_2Fe^{+/0}$, respectively, in 0.1 M tetrabutylammonium hexafluorophosphate ($TBAPF_6$) in MeCN consistent with previously reported values for the vanadium(V/IV) reduction potential.[50]

The electrochemical properties of **V-M** ($M = Na^+, K^+, Ba^{2+}, Nd^{3+}, La^{3+}$) were also measured in MeCN (Figure 2 and SI Figure S1) and values for the vanadium(V/IV) $E_{1/2}$ are listed in Table 2. The vanadium(V/IV) redox event for **V-Na**, **V-K**, and **V-Ba** is reversible and shifts anodically with increase of cation charge, consistent with the effect of incorporating charge with related heterobimetallic complexes previously investigated by the Yang group.[31–35] The same trend is observed in computed redox potentials, though the simple model used in the calculations overestimates the increase in $E_{1/2}$ as the cation charge increases (See SI for computational details and Table S2 for values). The vanadium(V/IV) reduction potential for the monocations (**V-Na** and **V-K**) shifts 90-130 mV more positive than **(salen)V(O)** and 114-164 mV more positive than **(salen-OMe)V(O)**. For the dication, **V-Ba**, the vanadium(V/IV) reduction potential shifts 440 mV positive of **(salen)V(O)** and 464 mV positive of **(salen-OMe)V(O)**. The cyclic voltammograms of **V-La** and **V-Nd** showed an irreversible oxidation event (E_{pa}) at 1.10 and 1.09 V vs $(C_5H_5)_2Fe^{+/0}$, respectively, indicating chemical instability of the vanadium(V) oxo for these complexes in MeCN. Attempts to isolate the lanthanum containing vanadium(V) oxo complex following chemical oxidation of **V-La** with $NOBF_4$ ($E^{o\prime}([NO]^+/NO)$ = 1.00 V vs $(C_5H_5)_2Fe^{+/0}$)[51] were unsuccessful. Differential pulse voltammetry (DPV) of **V-La** (See SI Figure S2) showed an additional oxidation feature directly following the vanadium(IV/V) oxidation (E_{pa} >1.3 V vs $(C_5H_5)_2Fe^{+/0}$) tentatively assigned as formation of the vanadium(V)-phenoxyl radical, in which the salen ligand is oxidized.[52,53] The closeness of these redox features (~200 mV) may contribute to the observed electrochemical and chemical instability in isolating the oxidized **V-La** species.

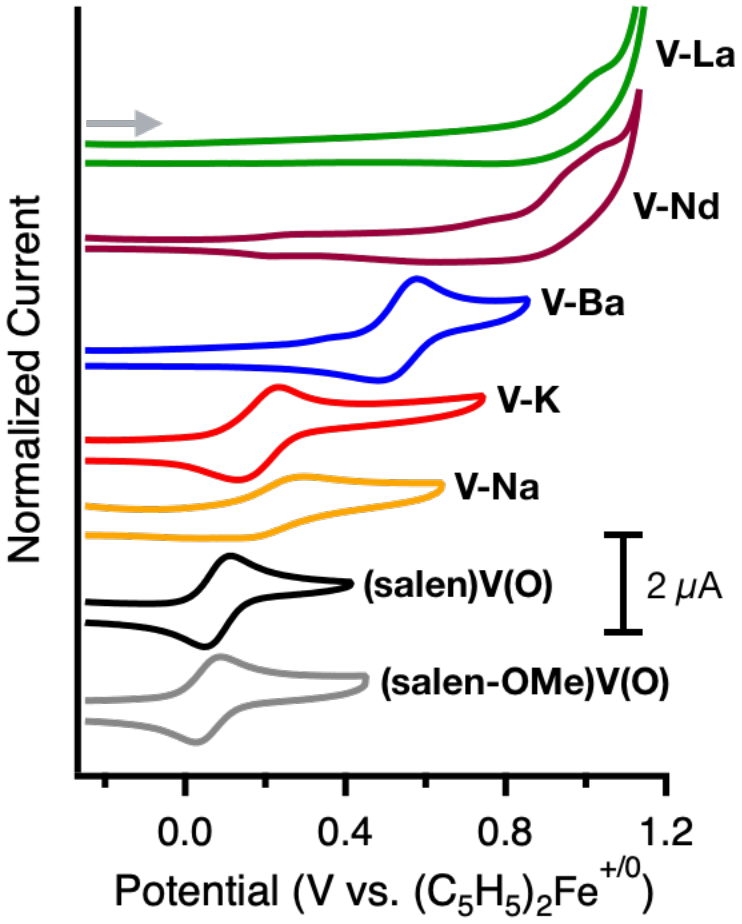

Figure 2. Cyclic voltammograms of **(salen)V(O)**, **(salen-OMe)V(O)**, and **V-M** (M = Na^+, K^+, Ba^{2+}, Nd^{3+}, and La^{3+}) (0.5 mM) in 0.1 M $TBAPF_6$ in MeCN under N_2. Scan rate is 100 mV/s. Decamethylferrocene ($((CH_3)_5C_5)_2Fe$) was used as internal reference and all potentials are reported vs. the $(C_5H_5)_2Fe^{+/0}$ redox couple.[54]

Table 2. Summary of electrochemical data for vanadyl complexes.

Complex	**$E_{1/2}$ V(V/IV) (V), MeCN[a]**	**$E_{1/2}$ V(V/IV) (V), DCM[a]**	**$E_{1/2}$ V(V/IV) (V), DMF[a]**	**pK_a of $M(OH_2)$ (aq.)[b]**	**log(K_{DMF})**
(salen)V(O)	0.090	0.045	−0.10	--	1.75
(salen-OMe)V(O)	0.066	–	−0.13	--	--
(salen-crown)V(O)	--	--	−0.12	--	--

V-Na	0.23	0.20	−0.050	14.8	--
V-K	0.18	--	−0.036	16.3	1.90
V-Ba	0.53	0.41	0.39, -0.11[c]	13.4	3.67
V-La	1.10[d]	0.78[d]	−0.16	9.06	7.42
V-Ce	--	--	−0.16	9.3	--
V-Nd	1.09[d]	--	--	8.4	--

[a] Reduction potentials referenced to $(C_5H_5)_2Fe^{+/0}$ couple. [b] Values from ref. [55]. [c] The redox events are quasireversible at all scan rates sampled, so in lieu of reporting $E_{1/2}$, the values reported here correspond to E_{pa} and E_{pc} potentials, for the irreversible oxidation and reduction events, respectively. [d] The redox event is irreversible, so the reported potentials correspond to an E_{pa} for the irreversible oxidation to the vanadium(V) species.

Cyclic voltammograms of **V-Na**, **V-Ba**, and **V-La** were measured in 0.1 M $TBAPF_6$ DCM solutions. All three complexes were sparingly soluble in DCM, which has a relatively low dielectric constant (ε) of 8.93. Shifts of 150 mV (**V-Na**), 365 mV (**V-Ba**) and 735 mV (**V-La**) more positive than **(salen)V(O)** were observed for the vanadium(V/IV) redox couple, correlating with the increase of cation charge (Table 2, see SI Figure S8). The vanadium(V/IV) couple for **V-K** and **V-Ba** appeared reversible, but **V-La** showed an irreversible oxidation, similar to its behavior in MeCN.

The electrochemical behavior of the vanadyl complexes as measured by cyclic voltammetry in 0.1 M $TBAPF_6$ DMF solutions was markedly different than that observed in either MeCN or DCM. The vanadium(V/IV) redox couple was relatively insensitive to cation bound in the crown, only varying 124 mV across the series compared to the >900 mV and >700 mV shifts observed in MeCN and DCM, respectively (Figure 3). Cyclic voltammetry of related heterobimetallic salen-crown complexes measured in DMF were previously shown to exhibit a positive shift in potential correlated with cation charge.[31,34] Therefore, we further probed the interaction of DMF at vanadium through electrochemical techniques (vide infra).

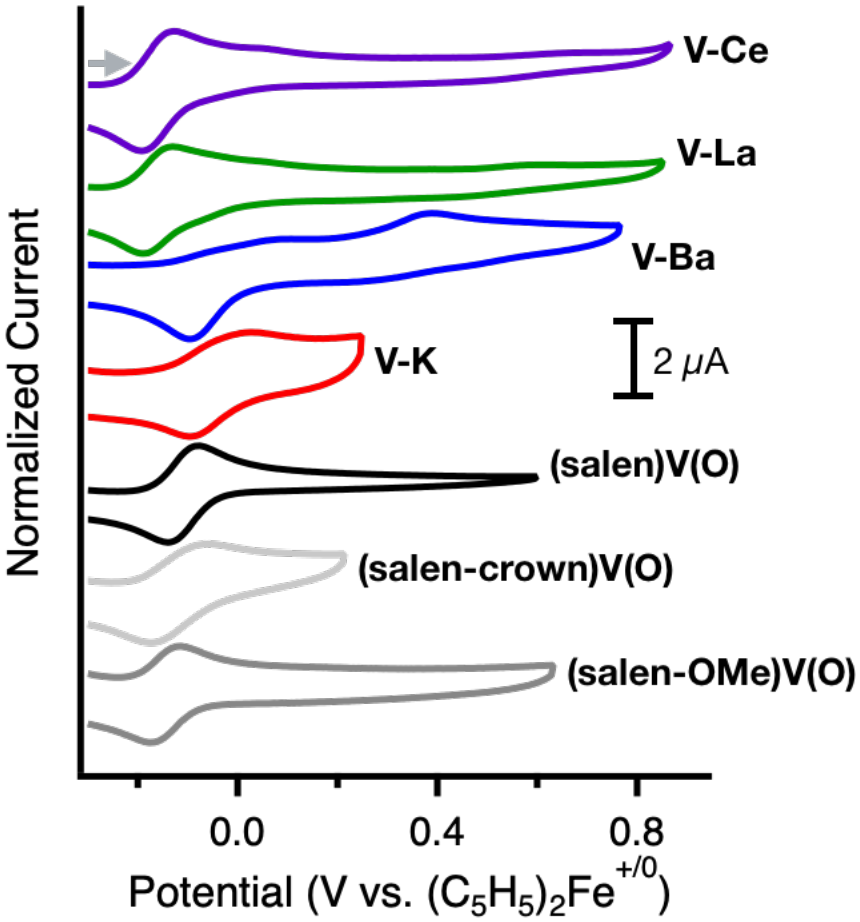

Figure 3. Cyclic voltammograms of **(salen)V(O)**, **(salen-OMe)V(O)**, **(salen-crown)V(O)**, and **V-M** (M = K^+, Ba^{2+}, La^{3+}, Ce^{3+}) (0.5 mM) in 0.1 M $TBAPF_6$ in DMF under N_2. Scan rate is 100 mV/s. Decamethylferrocene ($((CH_3)_5C_5)_2Fe$) was used as internal reference and all potentials are reported vs. the $(C_5H_5)_2Fe^{+/0}$ redox couple.

Previous electrochemical studies on vanadyl salen complexes show that solvent polarity and electrolyte interactions can greatly impact the redox behavior[50] and catalytic oxidation reactivity.[41,56–58] Square pyramidal vanadyl salen complexes possess an empty coordination site trans to the oxo group, and upon oxidation, the more electron deficient vanadium(V) typically favors a six-coordinate geometry instead of five. This empty coordination site can readily bind coordinating solvents or Lewis bases at the axial position.[59] Previous studies have investigated

association of weakly binding anions at this position.[60–62] Additionally, formation of dimeric or oligomeric chains with V–O–V–O linkages have been observed under acidic conditions.[63–66]

We looked to directly probe electrolyte, anion, and solvent interactions at the vanadyl salen-crown complexes in an attempt to better understand their behavior in DMF. Cyclic voltammograms of **V-K**, **V-Ba**, and **V-La** measured using the corresponding $M(OTf)_n$ (M^{n+} = K^+, Ba^{2+}, or La^{3+}) as electrolyte (200:1 electrolyte to analyte) in DMF again showed no clear trend in positive potential shift with increased cation charge (SI Figure S4). Cyclic voltammetry of **V-La** with 0.1 M tetrabutylammonium tetraphenylborate ($TBABPh_4$) electrolyte in DMF showed minimal difference on the vanadium(V/IV) reduction potential ($E_{1/2}$ = −0.16 V vs $(C_5H_5)_2Fe^{+/0}$). $TBABPh_4$ was chosen because it is a bulkier and relatively less coordinating electrolyte than $TBAPF_6$ or the $M(OTf)_n$ salts. The effect of anion dissociation in DMF was also explored as a reason for the lack of positive redox shift for **V-La** by cyclic voltammetry. Comparing reduction potentials of $[V\text{-}La][OTf]_3$ and $[V\text{-}La][Cl]_3$ in DMF with 0.1 M $TBABPh_4$ electrolyte showed no difference by cyclic voltammetry despite the chloride being a more strongly coordinating anion than triflate (SI Figure S5). The invariant reduction potentials under the different conditions explored indicate that another interaction must be responsible for the lack of positive shift in DMF.

The differences in the cyclic voltammograms of the vanadium complexes in MeCN versus DMF cannot be explained by dielectric constant of the solvent because the values are similar (ε = 37.5 and 36.7, respectively), and redox potentials computed with DFT and continuum solvent models are very similar for the two solvents (See SI for computational details). Instead, a better descriptor to consider is the differences in Lewis basicity of the solvents. The Gutmann donor number is a quantitative measure of Lewis basicity.[67–69] The donor numbers for MeCN (14.1 kcal/mol) and DMF (26.6 kcal/mol) correspond with the computed solvent molecule binding

energies, which are roughly twice as strong for DMF. Given that the vanadyl complexes offer several possible sites of interaction for a Lewis base, either at the vanadium center or through solvation of the Lewis acid cation, we experimentally determined binding constants for DMF. Cyclic voltammograms of the vanadyl complexes, **(salen)V(O)**, **V-K**, **V-Ba**, and **V-La**, were taken at varying concentrations of DMF in MeCN. In all cases, the vanadium(V/IV) reduction potential shifted cathodically with increasing concentrations of DMF (Figure 4). Further, for **V-La**, the redox couple became reversible at concentrations of 0.1 M DMF and above. This cathodic shift can be explained by DMF binding at the vanadium axial position, thus increasing electron density at the metal center and making it easier to oxidize vanadium(IV) to the vanadium(V) oxidation state. Binding constants for DMF ($\log(K_{DMF})$) were calculated using a modified form of the Nernst equation (eq 1), where a plot of $E_{1/2}$ vs log[DMF] gives a linear relationship.[70,71]

$$\Delta E_{1/2} = q\frac{0.0592}{n}\log[DMF] + \frac{0.0592}{n}\log(K_{DMF}) \quad (1)$$

In eq 1, q is the number of DMF molecules bound and n refers to the number of electrons involved in the redox event. For the one electron oxidation of vanadium(IV) to vanadium(V), the value of $\log(K_{DMF})$ increases as cation charge increases (Table 2). Further, the slope obtained from these data can be used to determine the number of DMF molecules bound. In the case of **(salen)V(O)**, there should be only one empty coordination site for DMF and the slope value of 0.05 V/decade is consistent with the binding of one molecule of DMF (See SI Figure S7). For the **V-M** complexes, the Lewis acidic metal cation provides an additional binding site. A similar analysis of the slopes for **V-K**, **V-Ba**, and **V-La** suggests that more than one molecule of DMF could be binding (q >1) (See SI). Therefore, binding of multiple DMF molecules at these complexes cannot be ruled out. Computed binding energies for the two possible binding sites (either V or K/Ba/La) for one DMF molecule suggest that for the **V-K** complex the two sites bind DMF equally strongly, and that for

V-Ba and **V-La**, the Ba/La cations bind DMF more strongly. Furthermore, DMF binding to either site reduces the DFT computed redox potential (e.g. for **V-K**, DMF binding reduces the reduction potential from 1.05 V to 0.85 V (vanadium-bound) or 0.84 V (potassium-bound). These calculations confirm that binding of multiple DMF molecules is a probable factor in determining the observed CV/titration behavior.

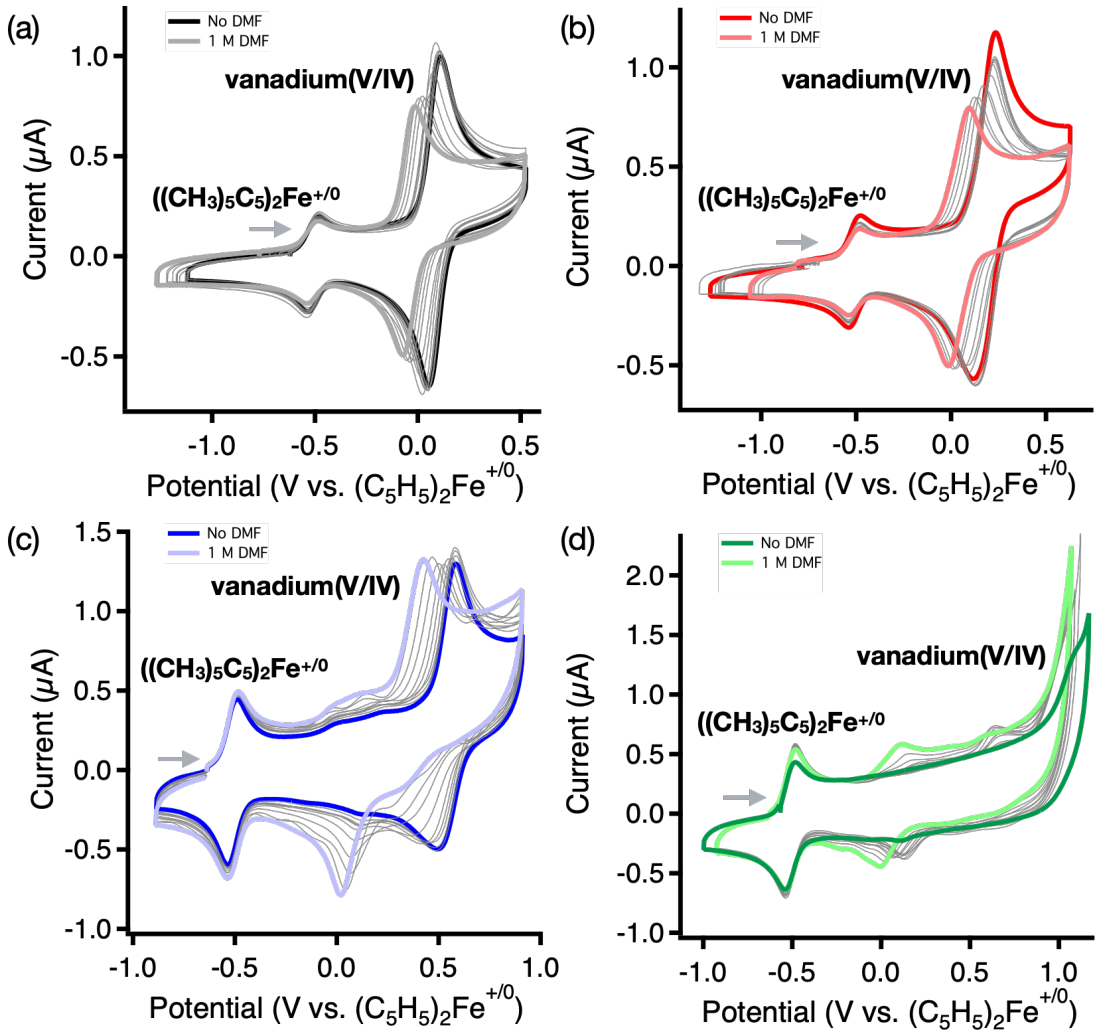

Figure 4. Cyclic voltammetry of (a) **(salen)V(O)**, (b) **V-K**, (c) **V-Ba**, (d) **V-La** with increasing titration of DMF. Scan rate at 100 mV/s in MeCN and 0.1 M $TBAPF_6$ electrolyte. Redox feature at $E_{1/2}$ = -0.51 V is decamethylferrocene ($((CH_3)_5C_5)_2Fe$) used as internal standard.

The interaction of Lewis acidic metals with the methoxy substituted complex, **(salen-OMe)V(O)**, was also explored. Interactions with salen vanadium oxo complexes with rare earth metals[72] and Group 14 and 15 Lewis acids[47] have previously been observed. Two different sites of interaction are possible – through the oxo group or through the methoxy substituents, more akin to the salen-crown complexes. A more electrophilic vanadyl center would disfavor association through the oxo unit. Cyclic voltammograms of **(salen-OMe)V(O)** were taken at different concentrations of $M(OTf)_n$ salt (M^{n+} = K^+, Ba^{2+}, La^{3+}) with 0.1 M $TBAPF_6$ in MeCN (Figure 5). The vanadium(IV/V) oxidation (E_{pa}) for **(salen-OMe)V(O)** shifted anodically in the presence of the exogenous $M(OTf)_n$ salts, where the maximum ΔE_{pa} observed was 0.082 V, 0.37 V, and 0.80 V for K(OTf), $Ba(OTf)_2$, and $La(OTf)_3$, respectively. However, the E_{pc} (vanadium(V/IV) reduction) of **(salen-OMe)V(O)** was shifted anodically by a smaller amount, where ΔE_{pc} was 0.069 V, 0.16 V, and 0.14 V for K(OTf), $Ba(OTf)_2$, and $La(OTf)_3$, respectively (Table 3). The asymmetry observed in the magnitude of the shift at the two redox features may be attributed to charge repulsion between the cationic vanadium(V) and the Lewis acidic metal, leading to a weaker association.

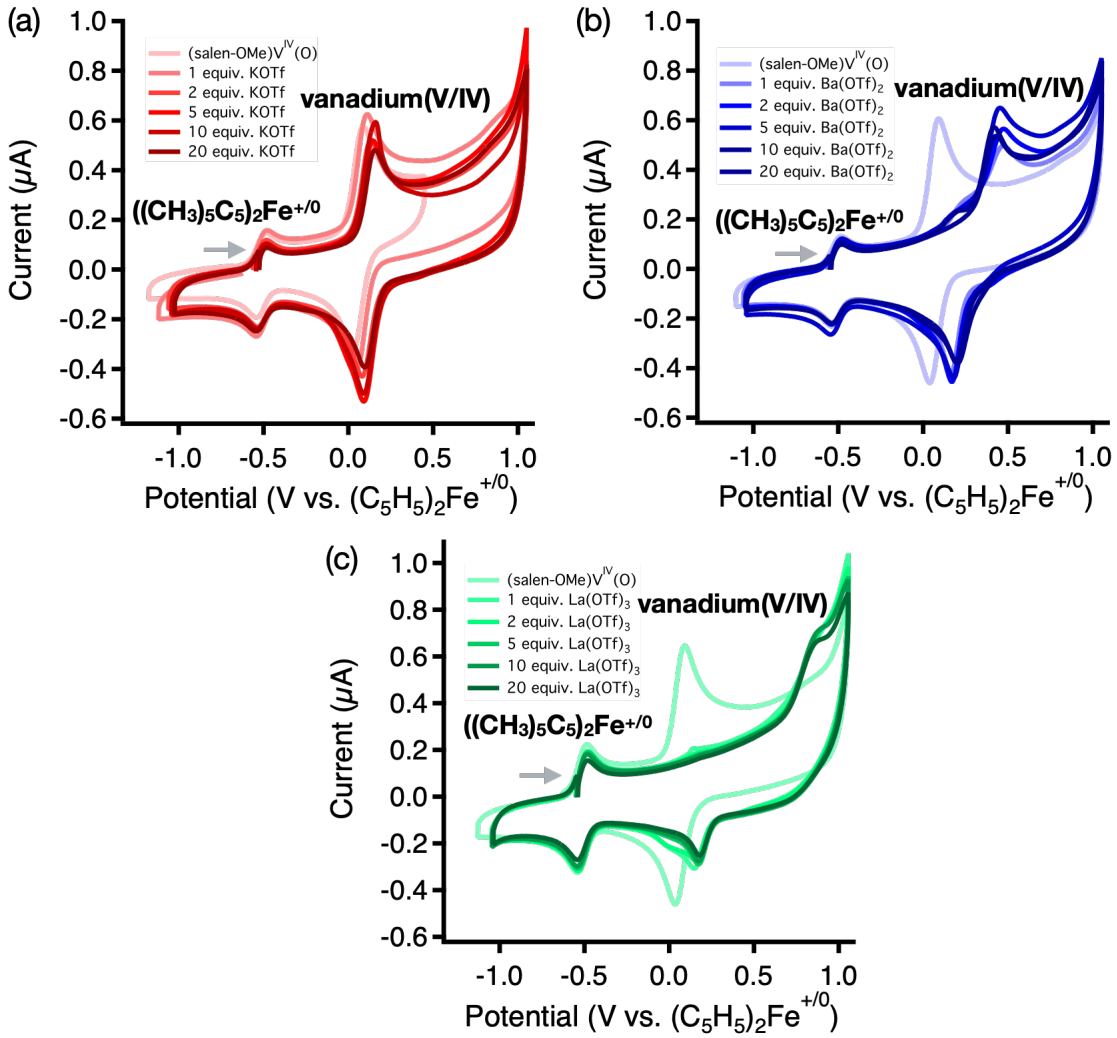

227

228 **Figure 5.** Cyclic voltammetry of **(salen-OMe)V(O)** with titration of (a) KOTf, (b) $Ba(OTf)_2$, or

229 (c) $La(OTf)_3$ salts. Scan rate at 100 mV/s in MeCN and 0.1 M $TBAPF_6$ electrolyte. Redox feature

230 at $E_{1/2}$ = -0.51 V is decamethylferrocene ($((CH_3)_5C_5)_2Fe$) used as internal standard.

231 **Table 3.** Summary of anodic and cathodic potential shifts from titration of **(salen-OMe)V(O)** with

232 $M(OTf)_n$ (M^{n+} = K^+, Ba^{2+}, La^{3+}) salts.[a]

Equiv. salt added	**K(OTf)**		**$Ba(OTf)_2$**		**$La(OTf)_3$**	
	ΔE_{pa} (V)	**ΔE_{pc} (V)**	**ΔE_{pa} (V)**	**ΔE_{pc} (V)**	**ΔE_{pa} (V)**	**ΔE_{pc} (V)**
0	0	0	0	0	0	0

1	0.020	0.014	0.37	0.12	0.79	0.11
2	0.025	0.030	0.37	0.13	0.79	0.12
5	0.045	0.051	0.37	0.14	0.80	0.14
10	0.058	0.058	0.33	0.16	0.79	0.14
20	0.082	0.069	0.32	0.16	0.79	0.14

[a] Reduction potentials referenced to $(C_5H_5)_2Fe^{+/0}$ couple. Potential shifts are reported relative to **(salen-OMe)V(O)** without $M(OTf)_n$ salt.

Electronic absorption and vibrational spectroscopy. The UV-visible spectra of the **V-M** complexes were explored in both MeCN and DMF (See SI for full spectra). Table 4 lists a summary of UV-visible spectroscopy. There are two major absorption bands observed for all complexes, with an intense band at ~360 nm corresponding to a mixed π–π*/charge transfer (CT) transition and a weaker band at ~580 nm corresponding to vanadium(IV) d-d transitions.[59] A slight red shift was observed in DMF for the π–π* band that was more pronounced for complexes containing a cation, and this shift may be due to stabilization by DMF coordination. Spectroelectrochemical UV-vis studies were also used to further investigate the stability of the vanadium complexes following oxidation in both MeCN and DMF. A controlled potential electrolysis ~200 mV positive of the vanadium(V/IV) reduction potential was applied in 0.2 M $TBAPF_6$ solutions and UV-vis spectra were collected at 1 second intervals during electrolysis. In MeCN, **(salen)V(O)**, **V-K**, **V-Ba** all showed the growth of a broad absorbance peak between 600-800 nm corresponding to a charge transfer band associated with formation of the vanadium(V) species (Figure S22). The UV-vis spectrum of **V-La** in MeCN under electrolysis only showed decomposition, further supporting the instability and inaccessibility of the vanadium(V) for the lanthanum containing complex. In DMF, however, the growth of the charge transfer band was observed for **V-K**, **V-Ba**, and **V-La**, indicating that bound DMF may be stabilizing the

vanadium(V) species, supporting the reversibility observed for the vanadium(V/IV) redox couple in DMF solutions (See SI Figure S23).

Table 4. Summary of electronic absorbance and vibrational spectroscopy.

Complex	**MeCN** λ**/nm (**ε**/M^{-1}cm^{-1})**	**DMF** λ**/nm (**ε**/M^{-1}cm^{-1})**	**υ(V≡O) (cm^{-1})**	**υ(C=N) (cm^{-1})**
(salen)V(O)	365 (9600), 590 (210)	363 (6075), 587 (123)[a]	968	1531
(salen-OMe)V(O)	360 (5600), 600 (200)	--	976	1522
(salen-crown)V(O)	--	376 (3400), 598 (110)	979	1525
V-Na	374 (2500), 592 (60)	378 (2990), 594 (70)	986	1554
V-K	374 (23,500), 584 (160)	376 (3900), 572 (90)	987	1553
V-Ba	366 (4400), 588 (70)	382 (5600), 578 (110)	989	1557
V-La	354 (4000), 610 (60)	378 (6300), 602 (170)	998	1563
V-Ce	354 (3900), 604 (170)	380 (9300), 592 (280)	1000	1564
V-Nd	346 (4700), 596 (180)	386 (3100), 598 (80)	994	1530

[a] Values from ref [73].

In vibrational spectroscopy, peak shifts can be observed in response to an electrostatic field. This is known as the vibrational Stark effect.[74] The solid-state infrared spectra for the vanadyl salen-crown complexes show that the V–O stretching frequency increases by 32 cm^{-1} and the imine C–N bond frequency increases by 42 cm^{-1} over the series of complexes. Plotting the vibrational data against the $E_{1/2}$ data collected in different solvents shows that a positive linear correlation is

present in MeCN and DCM consistent with a vibrational Stark effect, however in DMF no positive correlation is observed (Figure 6). The lack of positive correlation in DMF again may be a consequence of DMF binding to either the vanadium center or Lewis acidic metal cation.

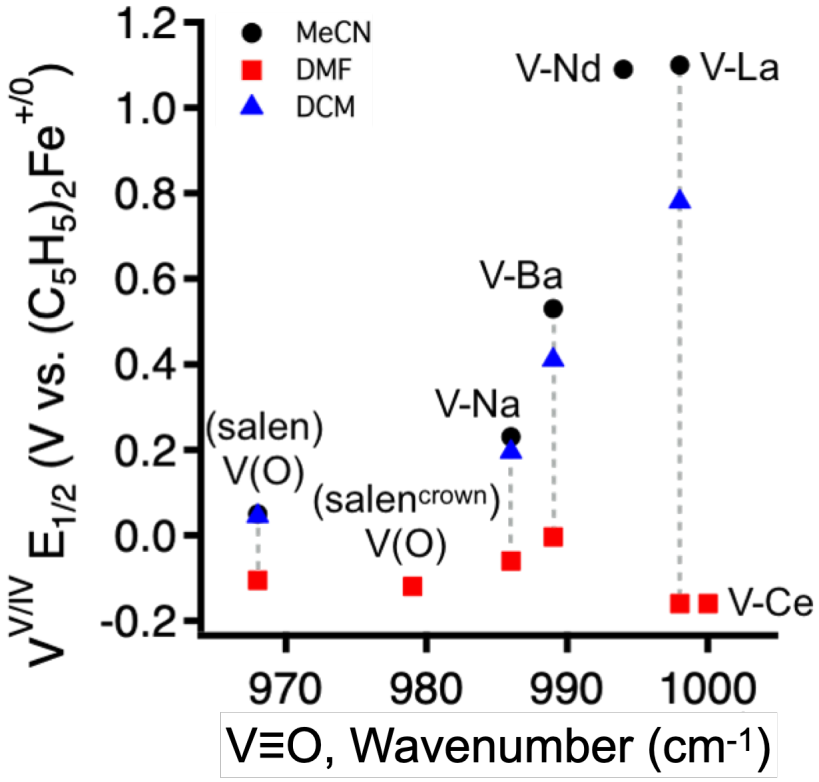

Figure 6. Plot showing vibrational Stark effect for vanadyl salen-crown complexes where there is a positive correlation between the V≡O stretching frequency and vanadium(V/IV) reduction potential in MeCN and DCM. However, this positive correlation is quenched in DMF, indicating electrostatic charge screening by DMF solvent.

CONCLUSIONS

These studies indicate that solvation effects and ability of DMF to act as a Lewis base can effectively quench electrostatic charge effects on reduction potentials. Cyclic voltammetry and UV-vis confirmed that DMF can act as a ligand and the binding constant increases as the cation charge increases and the metal center becomes more electron rich. In MeCN, incorporation of

charge leads to a shift in reduction potential for the vanadium(V/IV) couple by >900 mV. However, in DMF the reduction potential only shifts by 124 mV across the series of complexes investigated.

We have also demonstrated that addition of exogenous triflate salt to **(salen-OMe)V(O)** in MeCN produces a positive shift in the vanadium(V/IV) reduction potential, but charge repulsion upon oxidation to vanadium(V) results in cation dissociation and a loss of reversibility by cyclic voltammetry. The crown is essential for maintaining Lewis acid metal coordination and mitigating charge repulsion. The impact of these studies shows that electrostatic effects are dependent on solvent choice and coordination environment, informing future work on considering these interactions to avoid electric field quenching and improve catalyst design.

ASSOCIATED CONTENT

Supporting Information.

Experimental procedures and spectroscopic data (PDF)

V-K (CIF)

V-Ba (CIF)

V-La (CIF)

V-Nd (CIF)

V-Ce (CIF)

Computationally optimized geometries (ZIP)

AUTHOR INFORMATION

Corresponding Authors

*Nadia G. Léonard – leonarn1@uci.edu

*Anastassia Alexandrova – ana@chem.ucla.edu

Funding Sources

TC was supported by NSF Award #15554744 and NGL by NIH 3R01GM134047-02S1. NGL would also like to acknowledge support from the UC Presidential Postdoctoral Fellowship Program. J.Y.Y. also acknowledges support as a Sloan Foundation Fellow, a Canadian Institute for Advanced Research (CIFAR) Azrieli Global Scholar in the Bio-Inspired Solar Energy Program, and a Camille Dreyfus Teacher Scholar. A.N.A. acknowledges support from NSF CHE grant 22-3366. The authors acknowledge computational resources from the National Energy Research Scientific Computing Center (NERSC), a U.S. Department of Energy Office of Science User Facility located at Lawrence Berkeley National Laboratory, and DOE-BES grant DE-SC0019152.

REFERENCES

(1) Sutradhar, M.; Martins, L. M. D. R. S.; Guedes da Silva, M. F. C.; Pombeiro, A. J. L. Vanadium Complexes: Recent Progress in Oxidation Catalysis. *Coord. Chem. Rev.* **2015**, *301–302*, 200–239. https://doi.org/10.1016/j.ccr.2015.01.020.

(2) da Silva, J. A. L.; da Silva, J. J. R. F.; Pombeiro, A. J. L. Oxovanadium Complexes in Catalytic Oxidations. *Coord. Chem. Rev.* **2011**, *255* (19), 2232–2248. https://doi.org/10.1016/j.ccr.2011.05.009.

(3) Zhang, Y.; Holm, R. H. Vanadium-Mediated Oxygen Atom Transfer Reactions. *Inorg. Chem.* **1990**, *29* (5), 911–917. https://doi.org/10.1021/ic00330a005.

(4) Belokon, Y. N.; Maleev, V. I.; North, M.; Usanov, D. L. VO(Salen)(X) Catalysed Asymmetric Cyanohydrin Synthesis: An Unexpected Influence of the Nature of Anion X on the Catalytic Activity. *Chem. Commun.* **2006**, No. 44, 4614–4616. https://doi.org/10.1039/B609591G.

(5) Belokon, Y. N.; Clegg, W.; Harrington, R. W.; Maleev, V. I.; North, M.; Pujol, M. O.; Usanov, D. L.; Young, C. Mechanism-Guided Development of VO(Salen)X Complexes as Catalysts for the Asymmetric Synthesis of Cyanohydrin Trimethylsilyl Ethers. *Chem. Eur. J.* **2009**, *15* (9), 2148–2165. https://doi.org/10.1002/chem.200801679.
(6) Xi, W.; Liu, Y.; Xia, Q.; Li, Z.; Cui, Y. Direct and Post-Synthesis Incorporation of Chiral Metallosalen Catalysts into Metal–Organic Frameworks for Asymmetric Organic Transformations. *Chem. Eur. J.* **2015**, *21* (36), 12581–12585. https://doi.org/10.1002/chem.201501486.
(7) Gandeepan, P.; Müller, T.; Zell, D.; Cera, G.; Warratz, S.; Ackermann, L. 3d Transition Metals for C–H Activation. *Chem. Rev.* **2019**, *119* (4), 2192–2452. https://doi.org/10.1021/acs.chemrev.8b00507.
(8) Zhang, G.; Wu, J.; Zheng, S.; Neary, M. C.; Mao, J.; Flores, M.; Trovitch, R. J.; Dub, P. A. Redox-Noninnocent Ligand-Supported Vanadium Catalysts for the Chemoselective Reduction of C═X (X = O, N) Functionalities. *J. Am. Chem. Soc.* **2019**, *141* (38), 15230–15239. https://doi.org/10.1021/jacs.9b07062.
(9) Białek, M.; Leksza, A.; Piechota, A.; Kurzak, K.; Koprek, K. Oxovanadium(IV) Complexes with [ONNO]-Chelating Ligands as Catalysts for Ethylene Homo- and Copolymerization. *J. Polym. Res.* **2014**, *21* (4), 389. https://doi.org/10.1007/s10965-014-0389-4.
(10) Waidmann, C. R.; DiPasquale, A. G.; Mayer, J. M. Synthesis and Reactivity of Oxo-Peroxo-Vanadium(V) Bipyridine Compounds. *Inorg. Chem.* **2010**, *49* (5), 2383–2391. https://doi.org/10.1021/ic9022618.
(11) Radosevich, A. T.; Musich, C.; Toste, F. D. Vanadium-Catalyzed Asymmetric Oxidation of α-Hydroxy Esters Using Molecular Oxygen as Stoichiometric Oxidant. *J. Am. Chem. Soc.* **2005**, *127* (4), 1090–1091. https://doi.org/10.1021/ja0433424.
(12) Shi, M.; Xu, B. VO(Acac)2-Catalyzed Oxidative Coupling Reactions of Phosphonium Salts. *J. Org. Chem.* **2002**, *67* (1), 294–297. https://doi.org/10.1021/jo010616m.
(13) Ishikawa, T.; Ogawa, A.; Hirao, T. Oxovanadium(V)-Induced Oxidative Coupling of Organolithium and -Magnesium Compounds. *Organometallics* **1998**, *17* (26), 5713–5716. https://doi.org/10.1021/om980607c.
(14) Hirao, T. Vanadium in Modern Organic Synthesis. *Chem. Rev.* **1997**, *97* (8), 2707–2724. https://doi.org/10.1021/cr960014g.
(15) Galloni, P.; Conte, V.; Floris, B. A Journey into the Electrochemistry of Vanadium Compounds. *Coord. Chem. Rev.* **2015**, *301–302*, 240–299. https://doi.org/10.1016/j.ccr.2015.02.022.
(16) Tsuchida, E.; Yamamoto, K.; Oyaizu, K.; Iwasaki, N.; Anson, F. C. Electrochemical Investigations of the Complexes Resulting from the Acid-Promoted Deoxygenation and Dimerization of (N,N'-Ethylenebis(Salicylideneaminato))Oxovanadium(IV). *Inorg. Chem.* **1994**, *33* (6), 1056–1063. https://doi.org/10.1021/ic00084a015.
(17) Del Carpio, E.; Hernández, L.; Ciangherotti, C.; Villalobos Coa, V.; Jiménez, L.; Lubes, V.; Lubes, G. Vanadium: History, Chemistry, Interactions with α-Amino Acids and Potential Therapeutic Applications. *Coord. Chem. Rev.* **2018**, *372*, 117–140. https://doi.org/10.1016/j.ccr.2018.06.002.
(18) Pessoa, J. C.; Etcheverry, S.; Gambino, D. Vanadium Compounds in Medicine. *Coordination Chemistry Reviews* **2015**, *301–302*, 24–48. https://doi.org/10.1016/j.ccr.2014.12.002.
(19) Mjos, K. D.; Orvig, C. Metallodrugs in Medicinal Inorganic Chemistry. *Chem. Rev.* **2014**, *114* (8), 4540–4563. https://doi.org/10.1021/cr400460s.

(20) Muhammad, N.; Ali, S.; Shahzadi, S.; Khan, A. N. Oxovanadium(IV) Complexes of Non-Steroidal Anti-Inflammatory Drugs: Synthesis, Spectroscopy, and Antimicrobial Activity. *Russ J Coord Chem* **2008**, *34* (6), 448–453. https://doi.org/10.1134/S1070328408060109.
(21) Thompson, K. H.; Orvig, C. Coordination Chemistry of Vanadium in Metallopharmaceutical Candidate Compounds. *Coord. Chem. Rev.* **2001**, *219–221*, 1033–1053. https://doi.org/10.1016/S0010-8545(01)00395-2.
(22) Pessoa, J. C.; Correia, I. Salan vs. Salen Metal Complexes in Catalysis and Medicinal Applications: Virtues and Pitfalls. *Coord. Chem. Rev.* **2019**, *388*, 227–247. https://doi.org/10.1016/j.ccr.2019.02.035.
(23) Matsuoka, N.; Tsuchimoto, M.; Yoshioka, N. Theoretical Study of Magnetic Properties of Oxovanadium(IV) Complex Self-Assemblies with Tetradentate Schiff Base Ligands. *J. Phys. Chem. B* **2011**, *115* (26), 8465–8473. https://doi.org/10.1021/jp111779k.
(24) Matsuoka, N.; Kawamura, H.; Yoshioka, N. Magnetic Property and Crystal Structure of Bis [N-(4-Chlorophenyl) Salicylideneaminato] Oxovanadium (IV). *Chem. Phys. Lett.* **2010**, *488* (1), 32–37. https://doi.org/10.1016/j.cplett.2010.01.057.
(25) Takano, K.; Sunatsuki, Y.; Kojima, M.; Kinoshita, I.; Shibahara, T. Synthesis and Characterization of 8-Quinolinolato Vanadium(IV) Complexes. *Inorganica Chimica Acta* **2009**, *362* (9), 3201–3207. https://doi.org/10.1016/j.ica.2009.02.025.
(26) Papoutsakis, D.; Ichimura, A. S.; Victor G. Young, J.; Jackson, J. E.; Nocera, D. G. Structural and Magnetic Properties of Vanadyl Dichloride Solvates: From Molecular Units to Extended Hydrogen-Bonded Solids. *Dalton Trans.* **2004**, No. 2, 224–228. https://doi.org/10.1039/B309432D.
(27) Ishida, T.; Mitsubori, S.; Nogami, T.; Takeda, N.; Ishikawa, M.; Iwamura, H. Ferromagnetic Exchange Coupling of Vanadium(IV) Dπ Spins across Pyrimidine Rings: Dinuclear Complexes of Oxovanadium(IV) Bis(1,1,1,5,5,5-Hexafluoropentane-2,4-Dionate) Bridged by Pyrimidine Derivatives. *Inorg. Chem.* **2001**, *40* (27), 7059–7064. https://doi.org/10.1021/ic010730n.
(28) Castro, S. L.; Cass, M. E.; Hollander, F. J.; Bartley, S. L. Oxo-Vanadium(IV) Dimer of 3-Hydroxy-3-Methylglutarate: X-Ray Crystal Structure, Solid State Magnetism, and Solution Spectroscopy. *Inorg. Chem.* **1995**, *34* (2), 466–472. https://doi.org/10.1021/ic00106a008.
(29) Liu, Z.; Anson, F. C. Electrochemical Properties of Vanadium(III,IV,V)−Salen Complexes in Acetonitrile. Four-Electron Reduction of O2 by V(III)−Salen. *Inorg. Chem.* **2000**, *39* (2), 274–280. https://doi.org/10.1021/ic990958z.
(30) Chang, C. J.; Labinger, J. A.; Gray, H. B. Aerobic Epoxidation of Olefins Catalyzed by Electronegative Vanadyl Salen Complexes. *Inorg. Chem.* **1997**, *36* (25), 5927–5930. https://doi.org/10.1021/ic970824q.
(31) Reath, A. H.; Ziller, J. W.; Tsay, C.; Ryan, A. J.; Yang, J. Y. Redox Potential and Electronic Structure Effects of Proximal Nonredox Active Cations in Cobalt Schiff Base Complexes. *Inorg. Chem.* **2017**, *56* (6), 3713–3718. https://doi.org/10.1021/acs.inorgchem.6b03098.
(32) Chantarojsiri, T.; Ziller, J. W.; Yang, J. Y. Incorporation of Redox-Inactive Cations Promotes Iron Catalyzed Aerobic C–H Oxidation at Mild Potentials. *Chem. Sci.* **2018**, *9* (9), 2567–2574. https://doi.org/10.1039/C7SC04486K.
(33) Chantarojsiri, T.; Reath, A. H.; Yang, J. Y. Cationic Charges Leading to an Inverse Free-Energy Relationship for N−N Bond Formation by MnVI Nitrides. *Angew. Chem. Int. Ed.* **2018**, *57* (43), 14037–14042. https://doi.org/10.1002/anie.201805832.

(34) Kang, K.; Fuller, J.; Reath, A. H.; Ziller, J. W.; Alexandrova, A. N.; Yang, J. Y. Installation of Internal Electric Fields by Non-Redox Active Cations in Transition Metal Complexes. *Chem. Sci.* **2019**, *10* (43), 10135–10142. https://doi.org/10.1039/C9SC02870F.
(35) Léonard, N. G.; Chantarojsiri, T.; Ziller, J. W.; Yang, J. Y. Cationic Effects on the Net Hydrogen Atom Bond Dissociation Free Energy of High-Valent Manganese Imido Complexes. *J. Am. Chem. Soc.* **2022**, *144* (4), 1503–1508. https://doi.org/10.1021/jacs.1c09583.
(36) Léonard, N. G.; Dhaoui, R.; Chantarojsiri, T.; Yang, J. Y. Electric Fields in Catalysis: From Enzymes to Molecular Catalysts. *ACS Catal.* **2021**, 10923–10932. https://doi.org/10.1021/acscatal.1c02084.
(37) Weberg, A. B.; Murphy, R. P.; Tomson, N. C. Oriented Internal Electrostatic Fields: An Emerging Design Element in Coordination Chemistry and Catalysis. *Chem. Sci.* **2022**, *13* (19), 5432–5446. https://doi.org/10.1039/D2SC01715F.
(38) Hoffmann, N. M.; Wang, X.; Berkelbach, T. C. Linear Free Energy Relationships in Electrostatic Catalysis. *ACS Catal.* **2022**, *12* (14), 8237–8241. https://doi.org/10.1021/acscatal.2c02234.
(39) Brianese, N.; Casellato, U.; Tamburini, S.; Tomasin, P.; Vigato, P. A. Asymmetric Compartmental Macrocyclic Ligands and Related Mononuclear and Hetero-Dinuclear Complexes with d- and/or f-Metal Ions. *Inorganica Chimica Acta* **1999**, *293* (2), 178–194. https://doi.org/10.1016/S0020-1693(99)00235-2.
(40) Reath, A. H. Electrostatic Interactions in Heterobimetallic Complexes and Their Effect on Reduction Potentials, Electronic Structure, and Reactivity, UC Irvine, 2019. https://escholarship.org/uc/item/6h72z6hd#author (accessed 2021-07-02).
(41) Coletti, A.; Galloni, P.; Sartorel, A.; Conte, V.; Floris, B. Salophen and Salen Oxo Vanadium Complexes as Catalysts of Sulfides Oxidation with H2O2: Mechanistic Insights. *Catalysis Today* **2012**, *192* (1), 44–55. https://doi.org/10.1016/j.cattod.2012.03.032.
(42) Franceschi, F.; Solari, E.; Floriani, C.; Rosi, M.; Chiesi-Villa, A.; Rizzoli, C. Molecular Batteries Based on Carbon–Carbon Bond Formation and Cleavage in Titanium and Vanadium Schiff Base Complexes. *Chem. Eur. J.* **1999**, *5* (2), 708–721. https://doi.org/10.1002/(SICI)1521-3765(19990201)5:2<708::AID-CHEM708>3.0.CO;2-I.
(43) Fukuzumi, S.; Morimoto, Y.; Kotani, H.; Naumov, P.; Lee, Y.-M.; Nam, W. Crystal Structure of a Metal Ion-Bound Oxoiron(IV) Complex and Implications for Biological Electron Transfer. *Nature Chem.* **2010**, *2* (9), 756–759. https://doi.org/10.1038/nchem.731.
(44) Draksharapu, A.; Rasheed, W.; Klein, J. E. M. N.; Que Jr., L. Facile and Reversible Formation of Iron(III)–Oxo–Cerium(IV) Adducts from Nonheme Oxoiron(IV) Complexes and Cerium(III). *Angew. Chem. Int. Ed.* **2017**, *56* (31), 9091–9095. https://doi.org/10.1002/anie.201704322.
(45) Shannon, R. D. Revised Effective Ionic Radii and Systematic Studies of Interatomic Distances in Halides and Chalcogenides. *Acta Crystallographica Section A* **1976**, *32* (5), 751–767. https://doi.org/10.1107/S0567739476001551.
(46) Riley, P. E.; Pecoraro, V. L.; Carrano, C. J.; Bonadies, J.; Raymond, K. N. X-Ray Crystallographic Characterization of a Stepwise, Metal-Assisted Oxidative Decarboxylation: Vanadium Complexes of Ethylenebis[(o-Hydroxyphenyl)Glycine] and Derivatives. *Inorg. Chem.* **1986**, *25* (2), 154–160. https://doi.org/10.1021/ic00222a012.
(47) Cashin, B.; Cunningham, D.; Daly, P.; McArdle, P.; Munroe, M.; Ní Chonchubhair, N. Donor Properties of the Vanadyl Ion: Reactions of Vanadyl Salicylaldimine β-Ketimine and

Acetylacetonato Complexes with Groups 14 and 15 Lewis Acids. *Inorg. Chem.* **2002**, *41* (4), 773–782. https://doi.org/10.1021/ic010366s.
(48) Buckley, F.; Maryott, A. A.; Standards, U. S. N. B. of. *Tables of Dielectric Dispersion Data for Pure Liquids and Dilute Solutions*; U.S. Department of Comerce, National Bureau of Standards, 1958.
(49) Stelson, A. C.; Hong, C. M.; Groenenboom, M. C.; Little, C. A. E.; Booth, J. C.; Orloff, N. D.; Bergman, R. G.; Raymond, K. N.; Schwarz, K. A.; Toste, F. D.; Long, C. J. Measuring Ion-Pairing and Hydration in Variable Charge Supramolecular Cages with Microwave Microfluidics. *Commun Chem* **2019**, *2* (1), 1–10. https://doi.org/10.1038/s42004-019-0157-9.
(50) Galloni, P.; Coletti, A.; Floris, B.; Conte, V. Electrochemical Properties of VO Salen Complexes. *Inorganica Chimica Acta* **2014**, *420*, 144–148. https://doi.org/10.1016/j.ica.2013.12.019.
(51) Connelly, N. G.; Geiger, W. E. Chemical Redox Agents for Organometallic Chemistry. *Chem. Rev.* **1996**, *96* (2), 877–910. https://doi.org/10.1021/cr940053x.
(52) Kurahashi, T.; Fujii, H. One-Electron Oxidation of Electronically Diverse Manganese(III) and Nickel(II) Salen Complexes: Transition from Localized to Delocalized Mixed-Valence Ligand Radicals. *J. Am. Chem. Soc.* **2011**, *133* (21), 8307–8316. https://doi.org/10.1021/ja2016813.
(53) Clarke, R. M.; Herasymchuk, K.; Storr, T. Electronic Structure Elucidation in Oxidized Metal–Salen Complexes. *Coord. Chem. Rev.* **2017**, *352*, 67–82. https://doi.org/10.1016/j.ccr.2017.08.019.
(54) Aranzaes, J. R.; Daniel, M.-C.; Astruc, D. Metallocenes as References for the Determination of Redox Potentials by Cyclic Voltammetry Permethylated Iron and Cobalt Sandwich Complexes, Inhibition by Polyamine Dendrimers, and the Role of Hydroxy-Containing Ferrocenes. *Can. J. Chem.* **2006**, *84* (2), 288–299. https://doi.org/10.1139/v05-262.
(55) Perrin, D. D. *Ionisation Constants of Inorganic Acids and Bases in Aqueous Solution*; Elsevier, 2016.
(56) Menati, S.; Rudbari, H. A.; Khorshidifard, M.; Jalilian, F. A New Oxovanadium(IV) Complex Containing an O,N-Bidentate Schiff Base Ligand: Synthesis at Ambient Temperature, Characterization, Crystal Structure and Catalytic Performance in Selective Oxidation of Sulfides to Sulfones Using H2O2 under Solvent-Free Conditions. *J. Mol. Struc.* **2016**, *1103*, 94–102. https://doi.org/10.1016/j.molstruc.2015.08.060.
(57) Boghaei, D. M.; Mohebi, S. Synthesis, Characterization and Study of Vanadyl Tetradentate Schiff Base Complexes as Catalyst in Aerobic Selective Oxidation of Olefins. *J. Mol. Cat. A: Chem.* **2002**, *179* (1), 41–51. https://doi.org/10.1016/S1381-1169(01)00330-2.
(58) Gupta, K. C.; Sutar, A. K. Catalytic Activities of Schiff Base Transition Metal Complexes. *Coord. Chem. Rev.* **2008**, *252* (12), 1420–1450. https://doi.org/10.1016/j.ccr.2007.09.005.
(59) Kanso, H.; Clarke, R. M.; Kochem, A.; Arora, H.; Philouze, C.; Jarjayes, O.; Storr, T.; Thomas, F. Effect of Distortions on the Geometric and Electronic Structures of One-Electron Oxidized Vanadium(IV), Copper(II), and Cobalt(II)/(III) Salen Complexes. *Inorg. Chem.* **2020**, *59* (7), 5133–5148. https://doi.org/10.1021/acs.inorgchem.0c00381.
(60) Oyaizu, K.; Dewi, E. L.; Tsuchida, E. Coordination of BF4- to Oxovanadium(V) Complexes, Evidenced by the Redox Potential of Oxovanadium(IV/V) Couples in CH2Cl2. *Inorg. Chem.* **2003**, *42* (4), 1070–1075. https://doi.org/10.1021/ic0205987.

(61) Fairhurst, S. A.; Hughes, D. L.; Leigh, G. J.; Sanders, J. R.; Weisner, J. Novel Binuclear Vanadium(V)–Schiff Base Cations Containing Single Fluorine Bridges and the Structure of Difluorodioxovanadate(1–). *J. Chem. Soc., Dalton Trans.* **1994**, No. 18, 2591–2598. https://doi.org/10.1039/DT9940002591.
(62) Chatterjee, P. B.; Abtab, S. M. T.; Bhattacharya, K.; Endo, A.; Shotton, E. J.; Teat, S. J.; Chaudhury, M. Hetero-Bimetallic Complexes Involving Vanadium(V) and Rhenium(VII) Centers, Connected by Unsupported μ-Oxido Bridge: Synthesis, Characterization, and Redox Study. *Inorg. Chem.* **2008**, *47* (19), 8830–8838. https://doi.org/10.1021/ic800815p.
(63) Tsuchida, E.; Oyaizu, K. Oxovanadium(III–V) Mononuclear Complexes and Their Linear Assemblies Bearing Tetradentate Schiff Base Ligands: Structure and Reactivity as Multielectron Redox Catalysts. *Coord. Chem. Rev.* **2003**, *237* (1), 213–228. https://doi.org/10.1016/S0010-8545(02)00251-5.
(64) Yamamoto, K.; Oyaizu, K.; Tsuchida, E. Catalytic Cycle of a Divanadium Complex with Salen Ligands in O2 Reduction: Two-Electron Redox Process of the Dinuclear Center (Salen = N,N‘-Ethylenebis(Salicylideneamine)). *J. Am. Chem. Soc.* **1996**, *118* (50), 12665–12672. https://doi.org/10.1021/ja9617799.
(65) Oyaizu, K.; Yamamoto, K.; Yoneda, K.; Tsuchida, E. Multielectron Redox Process of Vanadium Complexes in Oxidation of Low-Coordinate Vanadium(III) to Oxovanadium(V) with Dioxygen. *Inorg. Chem.* **1996**, *35* (23), 6634–6635. https://doi.org/10.1021/ic960198h.
(66) Hills, A.; Hughes, D. L.; Leigh, G. J.; Sanders, J. R. Crystal and Molecular Structure of the Compound [(Salen) VOVO(Salen)][I5]·MeCN [Salen =N,N′-Ethylene-Bis(Salicylideneiminate)] and the Preparation of Similar Complexes with Other Schiff-Base Ligands. *J. Chem. Soc., Dalton Trans.* **1991**, No. 1, 61–64. https://doi.org/10.1039/DT9910000061.
(67) Gutmann, V. Solvent Effects on the Reactivities of Organometallic Compounds. *Coord. Chem. Rev.* **1976**, *18* (2), 225–255. https://doi.org/10.1016/S0010-8545(00)82045-7.
(68) *Solvents and Solvent Effects in Organic Chemistry*, 1st ed.; John Wiley & Sons, Ltd, 2010. https://doi.org/10.1002/9783527632220.
(69) Gritzner, G. Solvent Effects on Redox Potentials: Studies in N-Methylformamide. *J. Electroanal. Chem. Interfacial Electrochem.* **1983**, *144* (1), 259–277. https://doi.org/10.1016/S0022-0728(83)80160-0.
(70) Gangi, D. A.; Durand, R. R. Binding of Carbon Dioxide to Cobalt and Nickel Tetra-Aza Macrocycles. *J. Chem. Soc., Chem. Commun.* **1986**, No. 9, 697–699. https://doi.org/10.1039/C39860000697.
(71) *Electrochemical Methods: Fundamentals and Applications, 2nd Edition | Wiley*. Wiley.com. https://www.wiley.com/en-us/Electrochemical+Methods%3A+Fundamentals+and+Applications%2C+2nd+Edition-p-9780471043720 (accessed 2022-08-11).
(72) Costes, J.-P.; Dahan, F.; Donnadieu, B.; Garcia-Tojal, J.; Laurent, J.-P. Versatility of the Nature of the Magnetic Gadolinium(III)−Vanadium(IV) Interaction − Structure and Magnetic Properties of Two Heterobinuclear [Gd, V(O)] Complexes. *Eur. J. Inorg. Chem.* **2001**, *2001* (2), 363–365. https://doi.org/10.1002/1099-0682(200102)2001:2<363::AID-EJIC363>3.0.CO;2-A.
(73) Dutton, J. C.; Fallon, G. D.; Murray, K. S. Synthesis, Structure, ESR Spectra, and Redox Properties of (N,N’-Ethylenebis(Thiosalicylideneaminato))Oxovanadium(IV) and of Related

{S,N} Chelates of Vanadium(IV). *Inorg. Chem.* **1988**, *27* (1), 34–38. https://doi.org/10.1021/ic00274a009.
(74) Fried, S. D.; Boxer, S. G. Measuring Electric Fields and Noncovalent Interactions Using the Vibrational Stark Effect. *Acc. Chem. Res.* **2015**, *48* (4), 998–1006. https://doi.org/10.1021/ar500464j.